

POTENTIAL ENERGY SAVINGS WITH EXTERIOR SHADES IN LARGE OFFICE BUILDINGS AND THE IMPACT OF DISCOMFORT GLARE

Sabine Hoffmann¹, Eleanor Lee²

ABSTRACT

Exterior shades are highly efficient to reduce solar load in commercial buildings. Their impact on net energy use depends on the annual energy balance of heating, cooling, fan and lighting energy. This paper discusses the overall energy use intensity of various external shading systems for a prototypical large office building split into the different types of energy use and for different orientations and window sizes. Lighting energy was calculated for a constant lighting power as well as for dimmed lighting fixtures (daylighting control).

In section 3, slat angles and solar cut-off angles were varied for fixed exterior slat shading systems. While the most light-blocking shades performed best for the case without daylighting controls, the optimum cut-off angle with daylighting controls was found to be 30 deg for the used building prototype used in Chicago and Houston. For large window-to-wall (WWR) ratios, window related annual energy use could be reduced by at least 70 % without daylighting control and by a minimum of 86 % with daylighting control in average over all orientations.

The occurrence of discomfort glare was is considered in section 4 of the paper, which looks at the performance of commercially available exterior shading systems when an interior shade is used during those hours during which occupants would experience discomfort glare. Glare control impacts overall energy use intensity significantly for exterior shades with high transmittance, especially when daylighting controls are used. In these cases, exterior shades are only beneficial for window-to-wall areas ≥ 45 % in the hot Houston climate. For smaller windows and in a heating/cooling climate like Chicago exterior shades can increase energy consumption.

1. INTRODUCTION

In the attempt to save energy in commercial buildings, exterior shades are more and more frequently seen in new construction projects, and entire architectural trends are formed around the need to reduce solar load in the perimeter zones of high-rise buildings. Exterior shades, compared to other types of shading devices such as interior shades, between-pane shades or compared to electro-chromic glazing, are the most efficient way to reduce solar load because they block a large percentage of direct radiation before it hits the building envelope.

At times solar radiation can be very beneficial, for example when heating energy is needed. In office buildings, a significant benefit can be achieved by the visible light from the sun if there is a controlled lighting system installed which dims the electric lighting whenever the required illuminance level in the room can be fully or partially met by daylight (“daylighting control”). Therefore, blocking the sun

¹ Sabine Hoffmann, Lawrence Berkeley National Laboratory

² Eleanor Lee, Lawrence Berkeley National Laboratory

means a trade-off between heating, cooling, fan and lighting energy which has to be considered when making the decision for an exterior shade.

While there are established standards (e.g. NFRC [1]) and metrics (e.g. SHGC³) to determine the performance of glazing systems with various substrates and coatings, there are only few simple methods available to classify external shading systems like e.g. EN 13363 [2] which calculates an overall solar heat gain coefficient for slat shading systems including the glazing system. Classifying exterior shades is challenging because of their 2- or 3-dimensional geometry. Depending on the sun angle, the transmitted radiation and the heat transfer through a complex fenestration system (CFS) varies significantly over the course of the day and the course of the year, while the solar heat gain coefficient of a glazing system without shades does not show a major dependence on the solar incidence angle and is calculated for normal incidence.

While most building energy simulation programs have some capability of modeling blinds or simple shade geometries, the results presented here distinguish themselves from previous studies by the selection of the modeling tools used and the subsequent accuracy of the results. Furthermore it considers a long neglected aspect in the trade-offs related to exterior shades which is especially important in office buildings and which has mostly been excluded from building energy analysis so far: the occurrence of glare and the necessity to deploy an additional interior shade for glare control.

If office employees at work stations are disrupted in their work by high luminance levels from the façade, they are likely to pull the interior shade to reduce discomfort glare at their desks. Interior shades are only minimally efficient in reducing solar load because they block radiation only after it has entered the indoor space, but they reduce the availability of daylight significantly. The reduction of daylight is the actual purpose when using interior shades during glare conditions. Unfortunately, however, interior shades often remain deployed after the sun has moved out of direct sight, and the deployed shades keep reducing the daylight availability and the benefit of daylighting controls.

The accurate modeling of exterior shading devices and their impact on energy performance of a building requires a detailed representation of the geometric model in the simulation, the knowledge of the material surface properties (short-wave reflectance and transmittance, long-wave emittance), and the necessary simulation tools to calculate angle-dependent properties of the system and their impact on energy performance of the building. The aim of this work is therefore twofold: evaluate the potential of energy savings through exterior shades for large office buildings in a hot/cold (Chicago) and a hot/humid (Houston) climate and assess the variance of performance by modeling a variety of exterior shading systems which represent current practice in new construction and retrofit in combination with daylighting control and glare control.

³ SHGC: solar heat gain coefficient. SHGC defines the percentage of incident radiation which penetrates the interior space through the fenestration system either as transmitted radiation or as heat flux.

2. METHODS

2.1. Characterization of the complex fenestration systems

The twelve exterior shading systems assessed in this study were chosen to represent a wide range of exterior shades used in modern architecture as well as in retrofit projects. The combination of shading system and glazing system is called complex fenestration system (CFS) in the following.

2.1.1. Properties of the reference glazing and interior shade

The base glazing system is defined as a dual-pane, spectrally selective, low-e window with an outboard layer of low-iron, low-e glass ($e=0.018$) and an inboard layer of clear glass (system thickness: 24 mm). In the center of glass, the U-value of the glazing equals $1.4 \text{ W/(m}^2\text{K)}$ ($0.238 \text{ Btu/(h}\cdot\text{sf}\cdot\text{F)}$), the solar heat gain coefficient equals 0.30 and the visible transmittance is 0.39 (Table 1). Assuming a frame to window ratio of 15 %, the chosen base glazing would fulfill the prescriptive requirements of ASHRAE 90.1 (2013) [3] for vertical fenestration in all climates. For reference, in addition to the complex fenestration systems, all simulations were also run with the base glazing only, referred to as “no shade”.

In section 4 the base glazing and the CFS were modeled with an indoor, light gray ($R_{sol}=0.75$) fabric roller shade with an openness factor of 3% and diffusing properties to reduce discomfort glare. Performance values of the base glazing (and the CFS) with and without interior shade were calculated with LBNL Window 7 [4] and can be found in Table 1.

BASE GLAZING SYSTEM AND COMPLEX FENESTRATION SYSTEMS						
Name	Without interior shade			With interior shade		
	U-value [W/m ² K] COG	Solar Heat Gain Coefficient	Tvis	U-value [W/m ² K] COG	Solar Heat Gain Coefficient	Tvis
base glazing ("no shade")	1.4	0.30	0.65	1.2	0.17	0.09
shd 1	1.1	0.31	0.63	1.0	0.19	0.09
shd 2	1.1	0.18	0.34	0.9	0.11	0.05
shd 3	1.0	0.07	0.10	0.9	0.05	0.01
shd 4	1.1	0.05	0.06	0.9	0.04	0.01
shd 5	1.0	0.03	0.03	0.9	0.03	0.00
shd 6	1.0	0.08	0.12	1.0	0.07	0.02
shd 7a	1.0	0.10	0.18	1.0	0.08	0.07
shd 7b	1.0	0.09	0.12	1.0	0.09	0.02
shd 7c	1.0	0.09	0.13	1.0	0.08	0.03
shd 8	1.1	0.14	0.27	1.1	0.12	0.02
shd 9	1.0	0.10	0.17	1.0	0.08	0.05
shd 10	1.0	0.18	0.34	0.9	0.12	0.05

Table1: Performance values for base glazing and CFS based on Window7 calculations. All values are for the center of glass.

2.1.2. Description of the exterior shading systems

The range of modeled exterior shading systems comprises slat shading systems, louvers, meshes and an external roller shade. For the geometry of the investigated slat shading systems and the roller shade see Appendix A. All systems were modeled without mounts, with no connection to the window and at a distance to the outer glass layer typical for the class of shading system.

Opening factors according to ISO 15099 [5] account for the air flow between exterior shade and glazing systems. The long-wave emittance of the slat shading systems was calculated based on integrated hemispherical reflectance of the system using the emissivity of the slat material. The emittance of the meshes as well as their transmittance was measured at the LBNL optical lab [6] and the emittance of the interior roller shade was estimated based on material emissivity and front opening factor. Shade conductance was calculated as a weighted average of material conductivity and thermal conductivity of air, using the front opening multiplier as weighting factor. The material properties and simulation input values can be found in Appendix B, Table B1, B2.

2.1.2.1 Window screens – micro slat shading systems

Shd 1 – 5 are variations of a commercial window screen product [7] that is mainly used in retrofit projects. It attaches to the frame or to a separate support, and is usually mounted close to the window although it could be used at a greater distance to the façade as well. The screens are slat shading systems at a micro scale. Slat angles and the solar cut-off angles were varied by changing the ratio of width and spacing.

The advantage of this type of exterior shading systems is its low weight which reduces installation cost compared to heavier slat shading systems. As the added structural load is negligible, the screens are a good option for retrofit. Because of their microstructure the screens allow for a view to the outside. Drawbacks are aesthetic ones as the screen changes the appearance of the building and the shading system may impair the window cleaning unless it is removable.

2.1.2.2 Retractable and adjustable exterior shades

Shd 6 is an external roller shade made of stainless steel that rolls up into a casing on the window head powered by an electric motor [8]. The motor can be automated through control software or activated manually. It can be fully or partially retracted and allows therefore better control over solar radiation, daylight and glare. The lateral guard rail in which the roller shade moves secures it against wind loads and acts as an additional vertical shading fin.

Shd 7 is a retractable exterior shade including casing and guard rails with the additional option of adjusting the slat angle either manually or automated [9]. Depending on the width of the system the manufacturer guarantees a safe use of the deployed shade up to 15 – 22 m/s, which makes it a suitable product for high rise buildings. At wind speeds that exceed the recommended value the shade should be retracted. The manufacturing company offers a broad selection of finishes with different optical properties. Three variations were considered in this study: a highly reflective finish (shd 7a), a finish with low reflectance (shd 7b), and a finish that is promoted as being selective, i.e. a higher reflectance

in the visible spectrum than over the entire solar spectrum (shd 7c) (For reflectance values see Appendix B, Table B3).

The external roller shade and the retractable, adjustable slat shading system are more elaborate technologies, but also pricier than a fixed slat system. As with every motorized device, the risk of failure and subsequent need of replacement of movable parts raise the maintenance cost.

Both retractable shades were modeled as fixed and fully deployed exterior shading systems in this study.

2.1.2.3 Aluminum louvers

Shd 8 represents a common choice for fixed exterior shades: a flat oval shaped extruded aluminum louver that can be manufactured in any size and length and mounted at any horizontal or vertical angle and with any spacing between louvers. Aluminum louvers are most frequently used in up to five-story-buildings as their size and weight makes them susceptible to wind loads. In addition to macro scale louvers, smaller hollow aluminum blinds can also be found as inserts into shutters and sliding shades.

The variability of shape and size allows architects and engineers to optimize for design and/or performance and the breadth of possible manufacturers can help reduce cost. Attaching the support system for large louvers to the building requires special attention to avoid significant thermal bridges. The relatively high reflectance of aluminum (~ 0.7) will decrease over time with exposure to climate and dirt, and cleaning the louvers can prove challenging and/or cost intensive. The here considered shd 8 was modeled at a 45 deg angle with a solar cut-off angle of 30 deg.

Fig. 1: Examples of exterior shades on buildings



*Hilton Foundation, Agoura Hills
Stainless steel roller shade (shd 6)*



*Li Ka Shing, UC Berkeley campus
Aluminum louvers above window
Aluminum louvers in shutters (shd 8)*



*Federal Building, San Francisco
Metal mesh (similar to shd 10)*

2.1.2.4 Meshes and perforated metal sheets

Over the past 10 years the use of metal meshes on commercial or institutional buildings emerged as a new architectural trend. Metal meshes offer probably the largest range of products with almost any finish, geometry and opening factor possible. Perforated metal sheets with various perforation patterns are part of this class of fixed exterior shades which are usually used at a greater distance to the façade than most other exterior shades and which cover large parts of the building.

In addition to a specific metal mesh (shd 10) that is distributed in various shading applications [10], a less frequent polymer mesh (shd 9) [11] which is used in a similar way as the metal mesh has been modeled as well. The optical properties of both meshes have been measured as their delicate structure makes geometrical CAD modeling difficult.

2.1.3. Thermal and optical properties of the complex fenestration systems

The optical properties of complex fenestration systems depend on the incidence angle of the solar radiation. Therefore the geometries of shd 1–8 were modeled with Sketchup (see Appendix A), and the Radiance module Gen-BSDF was then used to describe the geometry of the shade in form of a bi-directional scattering function (BSDF) matrix. BSDF matrices attribute the corresponding transmittance and reflectance values (front and back) to 145 solar incidence angles. For materials with different reflection coefficients in the visible and the solar spectrum, Gen-BSDF was run for both ranges separately. The BSDF matrices of shd 9 (fabric mesh) and shd 10 (metal mesh) were measured at the Lawrence Berkeley National Laboratory [6].

The resulting BSDF matrices were then imported into Window 7 [4] as new entries in the shading layer database. The shading layers were added at the external side of the base glazing system described in 2.1.1. (For distance from glass and opening factor see Appendix B, Table B1). The resulting values for U-value, SHGC and T_{vis} under normal incidence can be found in Table 1. Window 7 generates also input files for the Klems-BSDF method in EnergyPlus [12].

2.1.4. Scalability

The simulation results of the modeled shading systems can be transferred approximately to larger sized slat shading systems with the same proportional geometry for the metric *Energy Use Intensity (EUI)*. In most exterior shading systems conductive heat transfer through the shade itself is negligible for the overall heat balance. The calculated convective heat transfer through the exterior shade is based on opening factors according to ISO 15099 in the simulation. The convective heat transfer between exterior shade and glazing system is treated separately and depends on the distance between the two. For high wind speeds and extreme conditions, computational fluid dynamics should be used for the assessment of convection through the shade and within the gap instead of the simplified approach applied here. The long-wave emittance of the shading system, the visible, and solar transmittance are fully scalable, i.e. the values remain the same if the geometrical relation stays the same but the dimensions are different.

2.2. Building energy simulation

2.2.1. Description of the commercial office building prototype

EnergyPlus building energy simulations were used to evaluate the performance of the exterior shading systems in a prototypical large office building. Building prototypes are often abstract, synthetic buildings, not real buildings, that have been developed for the purpose of being representative of a population of buildings of a given type; e.g., office, hospital, etc.. Data are collected on real buildings and these data are used to formulate a statistical representation of building construction, systems, and operations [13]. The US Department of Energy (DOE) has invested in the development of such prototypes over the past few decades and has made the prototypes publicly available for use by the building industry in order to standardize methods for evaluating technical measures and policies and to develop energy efficiency codes [14].

The original models are compliant with ASHRAE 90.1 and are available at a DOE website [15]. The parameters of the building prototype used for this study have been modified to be code compliant with the California building code Title 24 [16]. Variations of this model are now available at a California Energy Code website [17]. The results presented here were calculated with EnergyPlus version V8.1 (released Oct 28, 2013) because of some additional features described below in section 2.2.2 – 2.2.5..

The large office prototype was defined as a 12-story, 48 m high building with a rectangular floor plate that is 73 m (north-south) by 49 m (east-west) (Figure 2). Perimeter zones were 4.57 m deep, with a 2.7 m ceiling height and a floor-to-floor height of 4 m. The perimeter zones were oriented in the four cardinal directions: due north, east, south, and west. The window-to-exterior-wall ratio was varied from 0 to 0.60 in order to quantify performance as a function of window area. No exterior obstructions were modeled.

The office prototype was defined with significant internal loads. Occupant density was 9.3 m² floor area per person. Occupancy was primarily between the hours of 9:00 to 17:00 on weekdays. Equipment loads were 8.1 W/m². Lighting loads were 7.5 W/m² at 100 % and reduced according to available daylight level for the case with daylighting controls (see also: 2.2.3. *Scheduled Lighting Energy*).

The source or primary energy includes the added energy needed for transmission and distribution of energy from the utility. For natural gas, the site-to-source conversion factor is 1.1. For electricity, the conversion factor assumed for this study is 3.3. For this building type, lighting and HVAC (cooling, heating, reheat, fans and pumps of a variable air flow system (VAV)) account for more than the half of the energy end uses in commercial office buildings, and both are influenced by window and daylighting systems.

2.2.2. Scheduled Surface Gains

The accurate calculation of window heat gains through complex fenestration systems and their distribution over the surfaces of interior walls and ceiling requires first an angular description of the

CFS, and second it requires algorithms that consider the outgoing angle of direct radiation (out of the façade into the room). For this study, the absorbed energy has been calculated with Radiance, a research-grade ray tracing software [18], as hourly values over the whole year and the results are provided as external files. EnergyPlus accesses the values for absorbed radiation in the CFS layers and on the surfaces of the perimeter zone through a “schedule:file” object and the surfaces are referenced to these external files through newly introduced objects : “SurfaceProperty:SolarIncidentInside” and “ComplexFenestrationProperty: SolarAbsorbedLayers”. This method is a development of the LBNL window and daylighting group and was implemented into the official EnergyPlus release with version E+ V8.1.

2.2.3. Scheduled Lighting Energy

Similarly to the scheduled surface gains, lighting energy use with daylighting controls in this study is based on Radiance simulation results. During occupied hours (using the occupancy schedule of the large office prototype with the 2009 calendar year) the illuminance was kept to a design level (500 lux). The Radiance output represents the percentage of maximum lighting power density (W/m^2) that is needed to maintain the target illuminance. The use of relative lighting power density allows for lower design illuminance values (e.g. 300 lux) and can account for more efficient light fixtures. The daylight saving calculation is based on the assumption that the maximum lighting power density (EnergyPlus input value, here: 7.5 W/m^2) is capable to provide the design illuminance.

2.2.4. Glare Control with Energy Management System

Simulations of angular-selective systems [19] have shown the importance of daylight use for the total energy use of a building. According to the US Energy Information Administration, electric lighting energy accounts for 20 % of the site energy use in commercial buildings, and for 38 % of the electric energy [20]. In the simulation model used for our studies, angular-selective systems with higher transmission of visible light tend to lead to lower whole building energy consumption even if their cooling load is elevated. However, without consideration of glare the simulation results lack validity because systems with high visible transmittance or systems with a significant portion of direct radiation may produce glare which will make the occupants pull the interior shade, hence reduce the daylight availability.

In this study, a glare-based control algorithm was used based on Radiance results for Discomfort Glare Probability (DGP) and Discomfort Glare Index (DGI) to control the deployment of the interior shade. The Radiance glare calculations are run prior to the actual simulation and a scheduled control algorithm based on the hourly results for DGP and DGI is used for the actuation of the interior shade.

The simulation model represents a large office building with open space office area in the perimeter zone. Nine viewpoints (see Fig. 2) were used to evaluate the occurrence of glare and the degree of discomfort that it produces. As numerical limit when an interior shade has to be deployed because of glare, values of $\text{DGP} \geq 0.38$ or $\text{DGI} \geq 24$ for any of the viewpoints were chosen. The work-flow within the EnergyPlus simulation can be seen in Fig. 3.

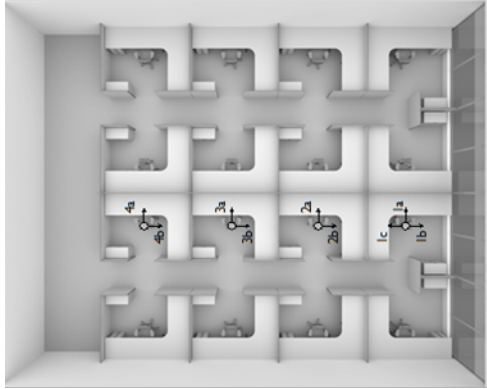


Fig. 2: Viewpoints of building model for glare evaluation

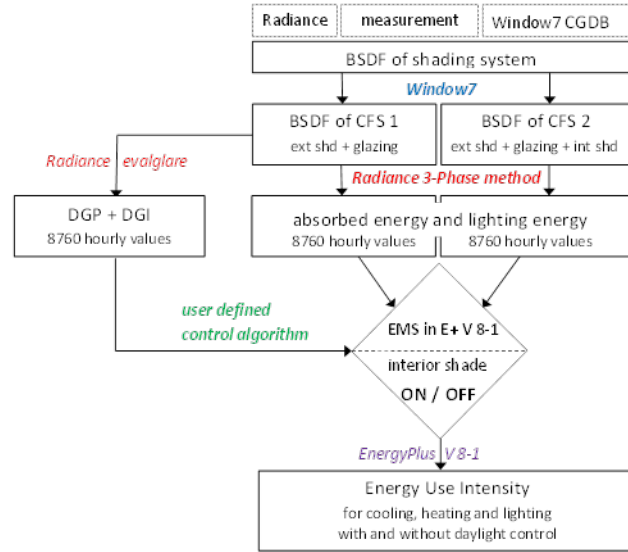


Fig. 3: Workflow in EnergyPlus

The Energy Management System (EMS) in EnergyPlus allows simulating an automated shading system based on any user defined control algorithm or schedule. With EnergyPlus V8-1 the possibility of using two shading layers (here: exterior and interior) and controlling them independently was implemented. Most building simulation programs do not allow for modeling two shading systems because of the interference of the scattering effect of shades or blinds. By adding two non-specular, scattering shading layer the problem shifts from a one-dimensional heat balance equation to a complex geometric calculation.

For the glare controlled simulation of exterior and interior shades, the “scheduled surface gains” method allowed use of the ray-tracing approach of Radiance and is therefore best suited to describe the optical properties of a façade system with multiple shading layers.

3. FIXED EXTERIOR SLAT SHADING SYSTEMS WITHOUT INTERIOR SHADE

In order to assess the impact of slat angle and cut-off angle for an exterior blind system with flat slats and a moderate reflectance ($R_{vis} = R_{sol} = 0.5$) the geometry of the commercially available product shd 2 was modified (see Table 2). The cut-off angle is defined as the highest profile angle at which direct radiation is transmitted into the space.

	shd 1	shd 2	shd 3	shd 4	shd 5
Slat angle (degree)	0	30	60	30	60
Cut-off angle (degree)	45	30	15	0	0
Ratio: slat width to spacing	1:1	1:1	1:1	1:0.5	1:0.86

Table 2: Variations of micro slat shading geometry

This section presents energy use intensity (EUI) in kWh/sf-yr of a 15 feet deep perimeter zone. A different trend for site vs. source energy can be related to the trade-off between admitted solar radiation, cooling and heating. A conversion factor site → source of 3.3 for electricity and of 1.1 for gas was assumed. Natural gas is used in the model to heat the hot water boiler which serves the central heating coil as well as the reheat coils. Reheat coils are also operating when parts of the building are in cooling mode, therefore gas usage does not exclusively indicate if it is used for heating or cooling.

The dark blue bar in the following Fig. 4 – 5 (Fig. 10 – 11) represents energy use that is not directly related to the window. It is based on simulation runs without any transparent area in the building envelope. The light grey bar is the energy use related to the window and the sum of dark blue and light grey is the total energy use as energy use intensity in kWh/sf-yr.

3.1. Without daylighting controls

Fig. 4 shows site and source energy for Chicago and Fig. 5 shows site and source energy for Houston for a relatively large window-to-wall ratio of 60 % (WWR 60) without daylighting control.

WWR 60, NDC, all orientations

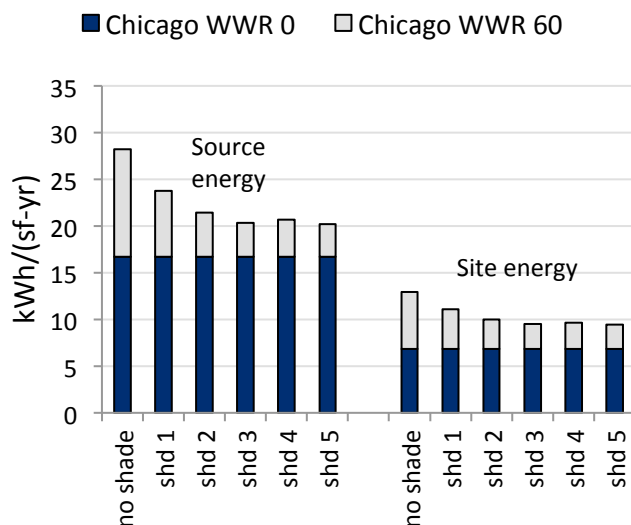


Figure 4: Source and site energy (HVAC and lighting) for a WWR of 60 % in Chicago without daylighting controls

WWR 60, NDC, all orientations

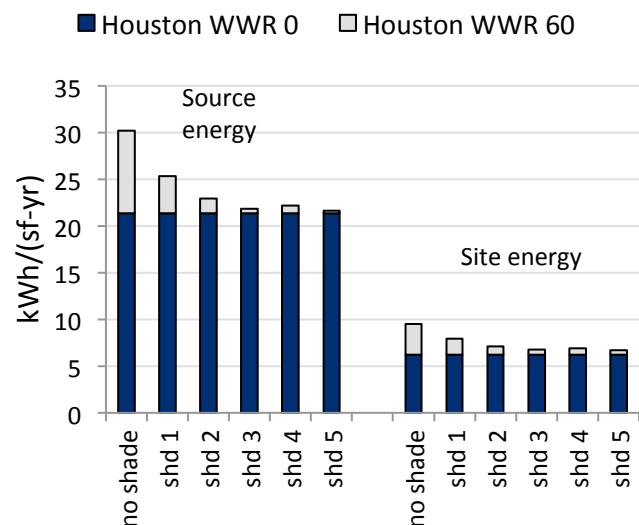


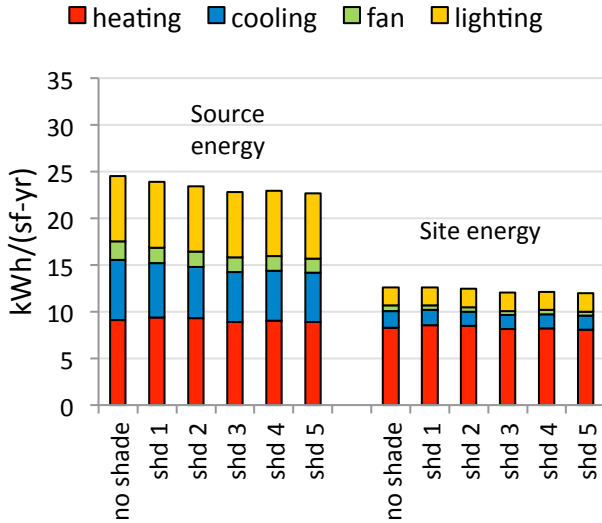
Figure 5: Source and site energy (HVAC and lighting) for a WWR of 60 % in Houston without daylighting controls

In both climates, Chicago and Houston, exterior shades reduce energy use intensity significantly. Shd 5 as best performing shade for the case without daylighting controls reduces total source energy use by 8.0 kWh/sf-yr (28 %) in Chicago and by 8.5 kWh/sf-yr (28 %) in Houston. This is a reduction of 70 % of the window related source energy for Chicago, and of 96 % in Houston.

Fig. 6-9 split site and source energy for Chicago and Houston into heating, cooling, fan and lighting for the four orientations of a perimeter zone. The energy quantities are disaggregated to

the different orientations according to the air flow of the VAV terminal units into the single zones. In this section results are shown for large windows with a WWR 60.

Chicago, WWR 60, NDC, north



Chicago, WWR 60, NDC, south

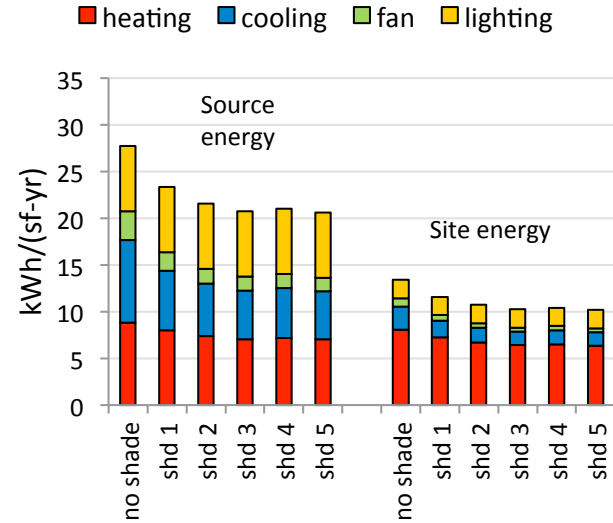
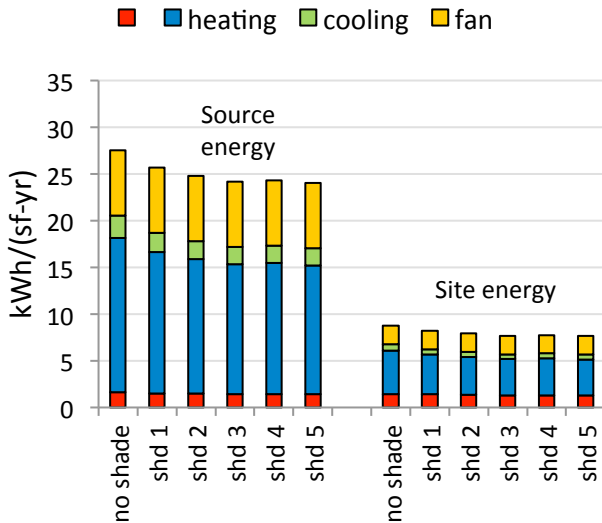


Figure 6: Source and site energy of a north oriented perimeter zone for heating, cooling, fan, lighting in Chicago without daylighting controls (WWR 60 %)

Figure 7: Source and site energy of a south oriented perimeter zone for heating, cooling, fan, lighting in Chicago without daylighting controls (WWR 60 %)

Houston, WWR 60, NDC, north



Houston, WWR 60, NDC, south

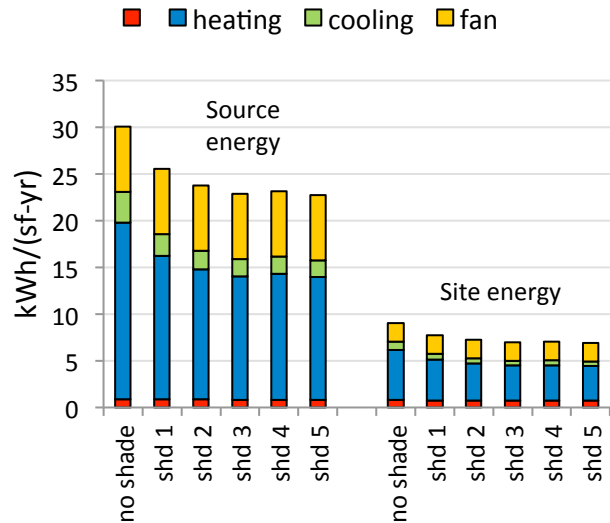


Figure 8: Source and site energy of a north oriented perimeter zone for heating, cooling, fan, lighting in Houston without daylighting controls (WWR 60 %)

Figure 9: Source and site energy of a south oriented perimeter zone for heating, cooling, fan, lighting in Houston without daylighting controls (WWR 60%)

In Chicago, heating energy is the main energy use for both, site and source energy. Heating energy that is used to meet heating loads is not significantly influenced by the exterior shades as

the EUI for heating on the north façade does not vary significantly. On the other hand, heating energy used for reheat during cooling is reduced by lower solar load for the cases with exterior shade on south, east and west façade.

In Chicago, of all orientations, the highest overall EUI without exterior shade can be found on the east façade with maximum values for both, heating and cooling. South and west façade show similar values with the south orientation requiring slightly more heating and fan energy than west orientation.

The best performing slat geometry is shd 5 for all orientations, and the highest absolute and relative reduction of total source energy can be achieved on the east façade where the source EUI is reduced by 10.9 kWh/sf-yr (34 %). For west and south orientation reductions are 6.1-7.1 kWh/sf-yr (23-26 %), and for north orientation a reduction of 1.8 kWh/sf-yr (7 %) was obtained.

In Houston, the energy use intensity for heating is small compared to cooling, fan, and lighting. Site and source energy follow therefore the same trend. Cooling is the predominant energy use and fan energy increases proportional to cooling energy. Highest EUI is found for east orientation with the west orientation following closely.

Like in Chicago, the best performing slat geometry in Houston is shd 5 for all orientations, and the absolute and relative reduction of total source energy on the east and west facade is 10.4-11.1 kWh/sf-yr (31-32 %). For south orientation a reduction of 7.4 kWh/sf-yr (24 %), and for north orientation savings of 3.5 kWh/sf-yr (13 %) were obtained.

3. 2. With daylighting controls

Fig. 10 and 11 show site and source energy for Chicago and Houston for a window-to-wall ratio of 60 % (WWR 60) and with daylighting controls. The light blue bars in the graph for Houston represent cases where total source energy (and in case of shd 2 - 5 even site energy) is below the non-window-related EUI. The white contours on top of the light blue bars represent the savings compared to a purely opaque wall. I.e. for a window-to-wall ratio of 60 % all exterior slat shading systems reduce source energy use intensity compared to the non-shaded case in Houston when averaged over all orientations.

WWR 60, DC, all orientations

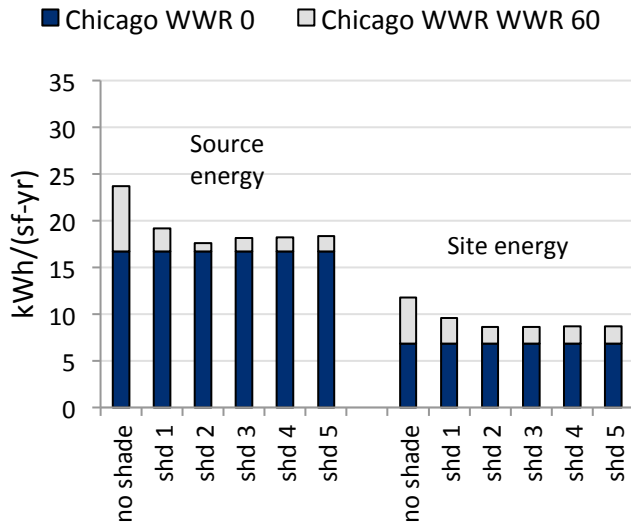


Figure 10: Source and site energy (HVAC and lighting) for a WWR of 60 % in Chicago with daylighting controls

WWR 60, DC, all orientations

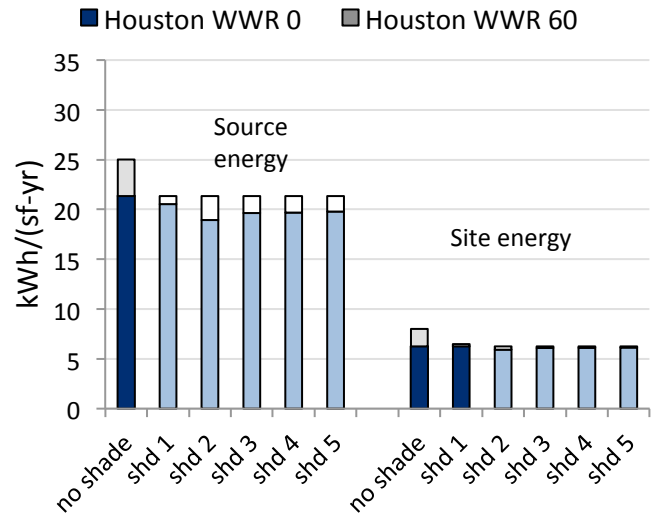


Figure 11: Source and site energy (HVAC and lighting) for a WWR of 60 % in Houston with daylighting controls

With daylighting control, shd 2 is the best performing shade in terms of source energy and reduces total source energy use by 6.1 kWh/sf-yr (26 %) in Chicago and by 6.1 kWh/sf-yr (24 %) in Houston. This is a reduction of 87 % of the window related source energy for Chicago, and a total elimination of window related heat gains in Houston.

Fig. 12 and 13 show the disaggregated energy use for north and south orientation for a window-to-wall ratio of 60 %.

While all exterior shades were beneficial to reduce source and site energy on any orientation when there were no daylighting controls assumed, the use of photosensors to dim artificial lighting when daylight is available changes this trend significantly. With daylighting controls, the only exterior shades that do not raise EUI in a north facing office are shd 1(Chicago, Houston) and shd 2 (Houston) with their relatively high cut-off angle $\geq 30^\circ$ (see Fig. 12 and 13).

In Chicago, when looking at the south façade, one can see the trade-off between cooling and lighting: the more blocking shades (shd 3 – 5) reduce cooling energy but require more lighting energy. While the sum of cooling and lighting energy is smaller for shades with higher cut-off angle, an increase in reheat energy due to higher cooling loads offsets this advantage (see e.g. shd 1, east orientation, Fig. 11d).

In Houston, where cooling energy is predominant and heating energy comparatively small, there is still an advantage of less blocking shades (except for shd 1 on east orientation). Shd 2 shows the optimum ratio of blocking solar radiation and admitting daylight.

Maximum reductions for Chicago are 8.7 kWh/sf-yr (34 %) for east, 5.5 kWh/sf-yr (25 %) for south, and 3.9 kWh/sf-yr (19 %) for west orientation. In Houston maximum reductions are 8.2 kWh/sf-yr (30 %) for east, 4.8 kWh/sf-yr (21 %) for south, and 7.4 kWh/sf-yr (27 %) for west orientation.

Chicago, WWR 60, DC, north

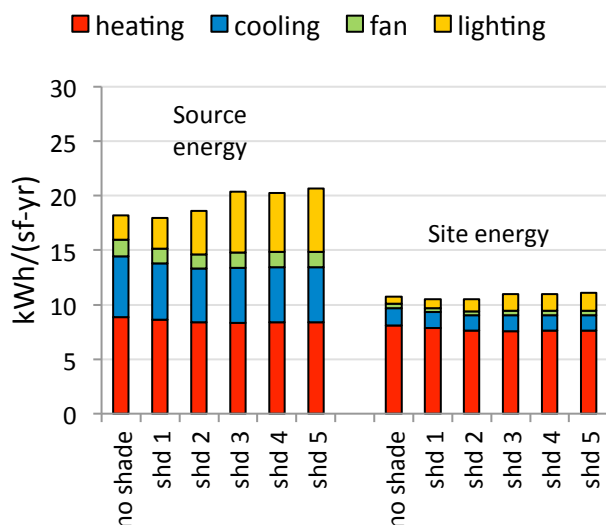


Figure 12: Source and site energy of a north oriented perimeter zone for heating, cooling, fan, lighting in Chicago with daylighting controls (WWR 60 %)

Chicago, WWR 60, DC, south

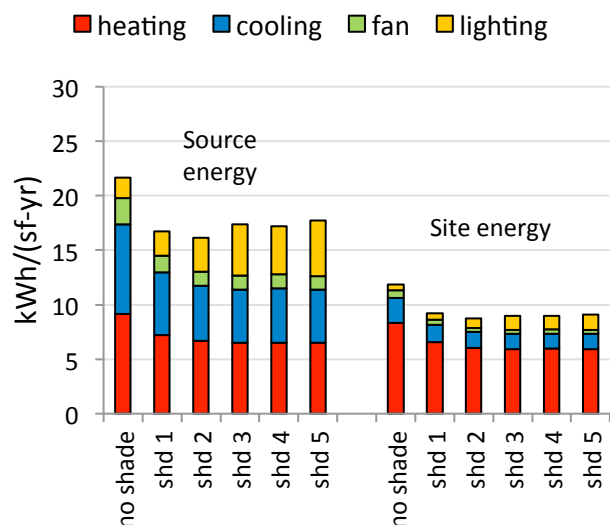


Figure 13: Source and site energy of a south oriented perimeter zone for heating, cooling, fan, lighting in Chicago with daylighting controls (WWR 60 %)

Houston, WWR 60, DC, north

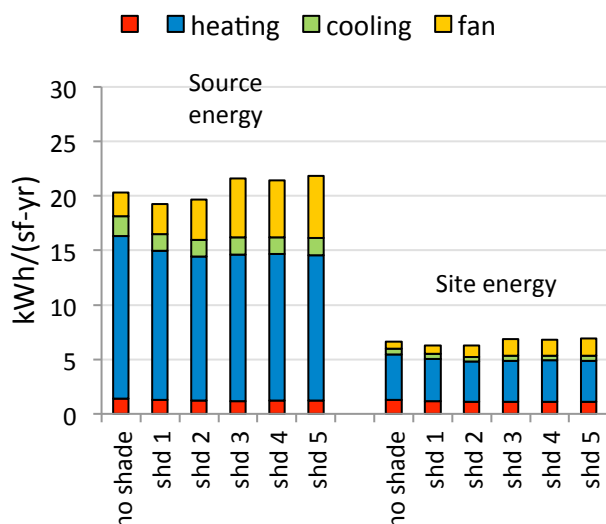


Figure 14: Source and site energy of a north oriented perimeter zone for heating, cooling, fan, lighting in Houston with daylighting controls (WWR 60 %)

Houston, WWR 60, DC, south

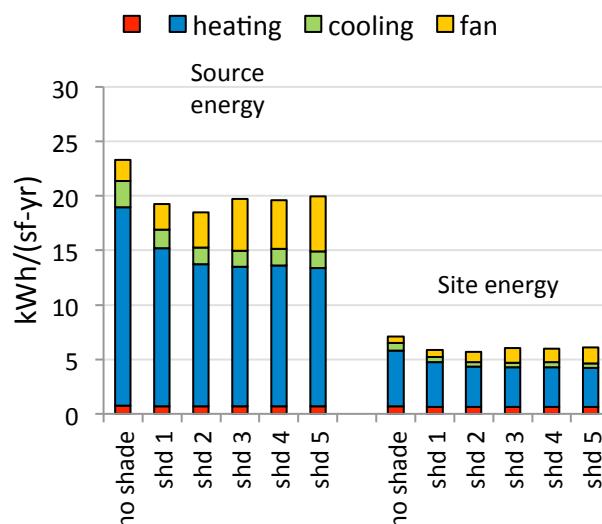


Figure 15: Source and site energy of a south oriented perimeter zone for heating, cooling, fan, lighting in Houston with daylighting controls (WWR 60 %)

4. INFLUENCE OF GLARE ON ENERGY USE INTENSITY

The previous section 3 did not consider the possibility of discomfort glare. Not only can direct radiation from the sun lead to discomfort glare, but indirect light that is reflected from the shade into the room may also contribute to a situation where visual comfort at a workstation cannot be maintained without the use of an interior shade. The probability of glare conditions in the perimeter zone of an office building depends on the geometry of the shade, on the cut-off angle in the case of slat shading systems, and on the reflectance and transmittance of its material.

Table 3 shows the frequency of glare occurrence as well as the number of hours during which the interior shade is pulled, based on the assumption that it stays down for the rest of the day. With most shades, west and east orientation experience the most frequent glare conditions because of the low solar incidence angle. Based on the assumed behavior (shade stays down for the rest of the day) the number of hours with shade down is significantly higher for east orientation than for west orientation.

Table 3 highlights the case without exterior shade and the five shades with the highest number of hours during which discomfort glare was calculated for one of the viewpoints (for viewpoints see Fig. 2 in 2.2.4.). Most frequently glare occurs for the base glazing without exterior shade. Shd 1, shd 2, shd 8 (aluminum louvers: $R_{vis} = R_{sol} = 0.7$, slat angle of 45 deg, cut-off angle of 30 deg), and shd 9 and shd 10 (perforated screens) are the shades with the highest number of glare occurrence.

Name	Number of hours with discomfort glare for one of the viewpoints						Number of hours with interior shade deployed					
	Chicago			Houston			Chicago			Houston		
Name	East	South	West	East	South	West	East	South	West	East	South	West
no shade	3298	3296	3308	3581	3480	3550	5999	5799	5587	5944	3296	5567
shd 1	3314	2906	3328	3594	3224	3583	5991	5789	5618	5937	2906	5596
shd 2	951	1150	1003	1021	937	1145	4647	3388	3027	5053	1150	3174
shd 3	67	0	78	53	0	88	1160	0	596	884	0	723
shd 4	0	0	0	0	0	0	0	0	0	0	0	0
shd 5	0	0	0	0	0	0	0	0	0	0	0	0
shd 6	114	2	121	98	0	136	1910	38	927	1636	2	1042
shd 7a	515	471	519	505	307	581	3306	1764	1906	3274	471	2224
shd 7b	265	69	287	230	3	286	3084	398	1549	2824	69	1751
shd 7c	273	74	255	230	20	266	3137	408	1490	2680	74	1678
shd 8	800	824	871	868	599	947	4256	2366	2685	4755	824	2874
shd 9	729	700	775	721	531	829	4017	2045	2466	4266	700	2692
shd 10	1043	1368	1113	1139	1154	1234	4759	3984	3154	5114	1368	3287

Table 3: Frequency of glare and frequency of interior shade deployment, highlighted are the systems that are shown in Fig.17 – 20, window-to-wall ratio 60%

To assess the impact of discomfort glare and the use of an interior shade to avoid it, this section contains results for all exterior shading systems with and without glare control for both cases, with and without daylighting controls installed. In the following figures, the source energy use intensity of a prototypical large office building with exterior shades is compared to a code compliant Ashrae 90.1 building without exterior shades. EUI is shown for source energy over four different window-to-wall ratios. Intermediate WWRs are interpolated. The red numbers in the graphs show the percentage savings that the best performing shading system achieves for a given window-to-wall ratio (0, 15, 30, 45, 60 %).

Code reference EUI:

The base glazing (see Table 1) without exterior shade is used as reference curve for code compliance. The dark gray area represents EUI values of 50 % of the code reference value or less. As ASHRAE 90.1 requests a limitation of WWR to 40 % for the standard model, the code EUI (and subsequently the 50 % code EUI) was capped at WWR 45⁴. No glare control was assumed for the code reference case, so the reference line remains the same whether glare control was assumed or not. Daylighting controls were modeled for the reference case in 4.2. *With daylighting control.*

4.1. Without daylighting control

Without daylighting control, the energy savings compared to the code reference EUI range from 14 % - 21 % in Chicago, and from 19 % - 26 % in Houston. Without glare control, maximum savings are 1-2 % higher than with glare control for the best performing shades. The best performing shades are shd 5, shd 6, shd 7b and shd 7c for both climates, Chicago and Houston.

Shd 1 shows the least improvement compared to the reference case and even exceeds code EUI for large windows with glare control in Chicago. Shd 2 and shd 10 are close to the best performing shades without glare control, but when applying glare control their energy savings are small compared to shd 3 – 9 which do not show a significant spread amongst them.

The slope of the EUI curve for exterior shades is much smaller than the slope of the reference EUI (until the capping) which means that window related energy use increases only moderately with increasing window-to-wall ratio.

⁴ The window-to-wall ratios of the building model were varied in 15% increments (15%, 30%, 45%, 60%) while the ASHRAE limit is set to 40%. An additional model with a WWR 40% was not generated for convenience.

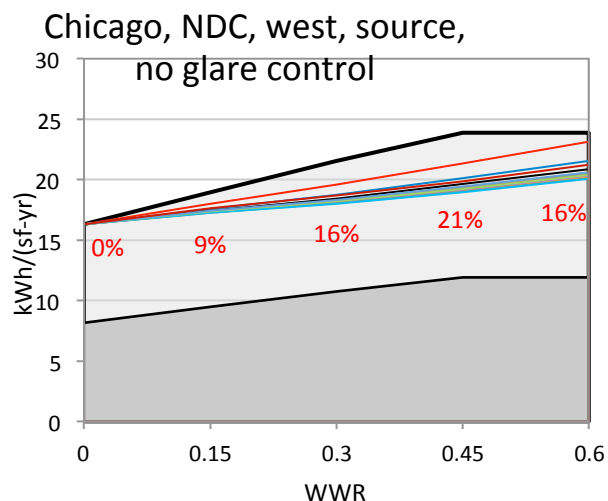


Figure 16: Total source EUI over WWR for all 12 exterior shades in Chicago, west orientation, without daylighting control, without glare control. Code reference line is capped at WWR 45 %.

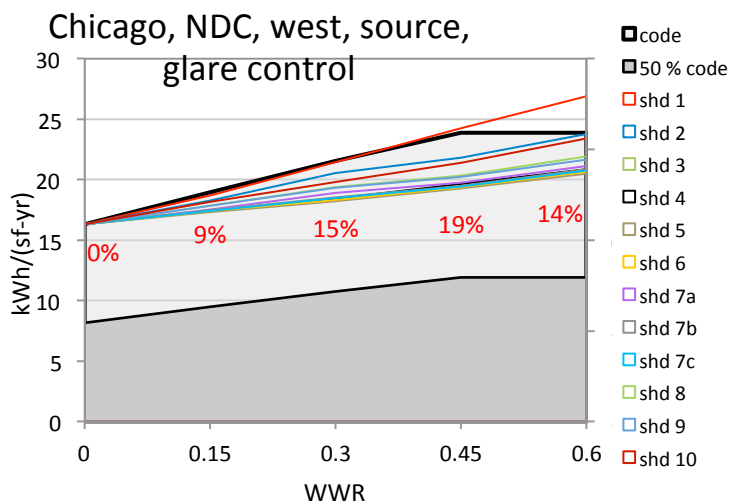


Figure 17: Total source EUI over WWR for all 12 exterior shades in Chicago, west orientation, without daylighting control, with glare control. Code reference line is capped at WWR 45 %.

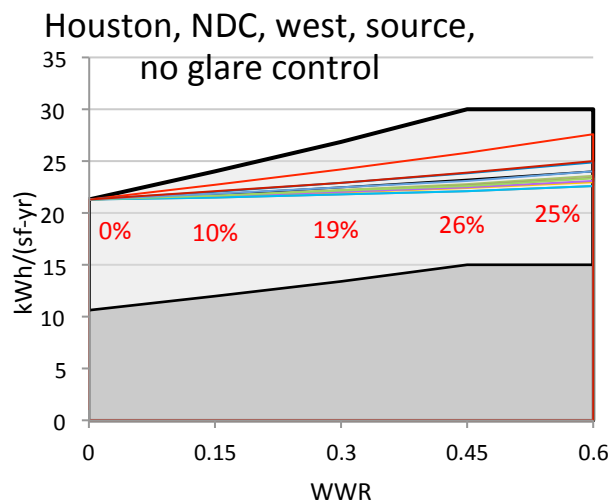


Figure 18: Total source EUI over WWR for all 12 exterior shades in Houston, west orientation, without daylighting control, without glare control. Code reference line is capped at WWR 45 %.

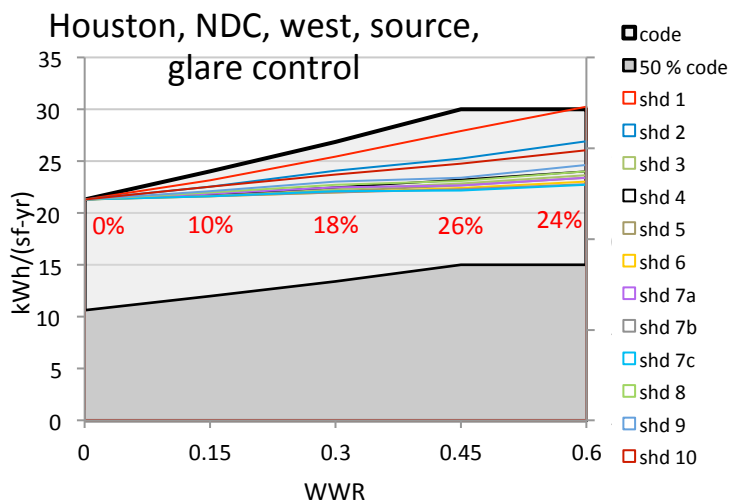


Figure 19: Total source EUI over WWR for all 12 exterior shades in Houston, west orientation, without daylighting control, with glare control. Code reference line is capped at WWR 45 %.

4.2. With daylighting control

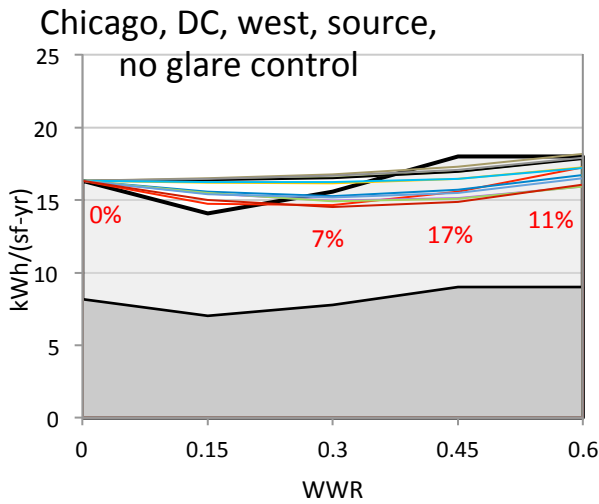


Figure 20: Total source EUI over WWR for all 12 exterior shades in Chicago, west orientation, with daylighting control, without glare control. Code reference line is capped at WWR 45 %.

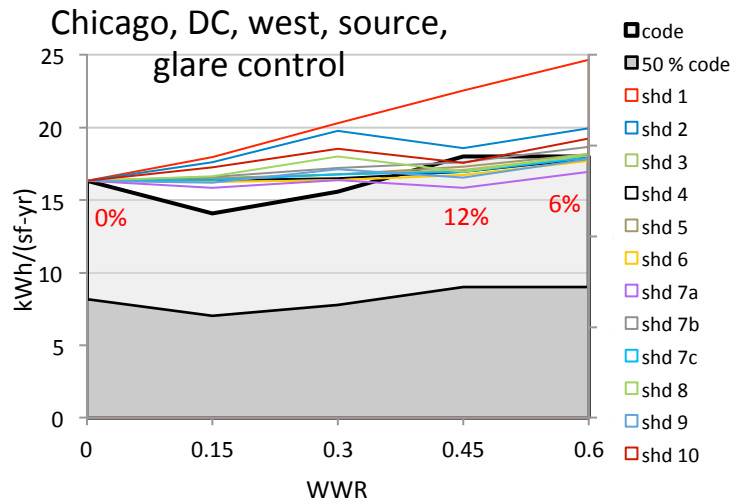


Figure 21: Total source EUI over WWR for all 12 exterior shades in Chicago, west orientation, with daylighting control, with glare control. Code reference line is capped at WWR 45 %.

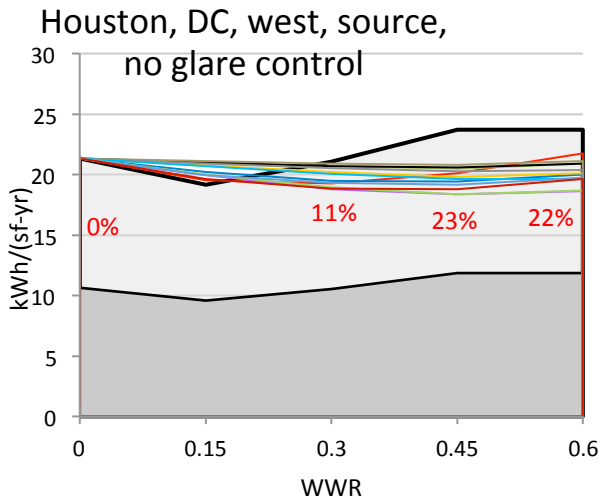


Figure 22: Total source EUI over WWR for all 12 exterior shades in Houston, west orientation, with daylighting control, without glare control. Code reference line is capped at WWR 45 %.

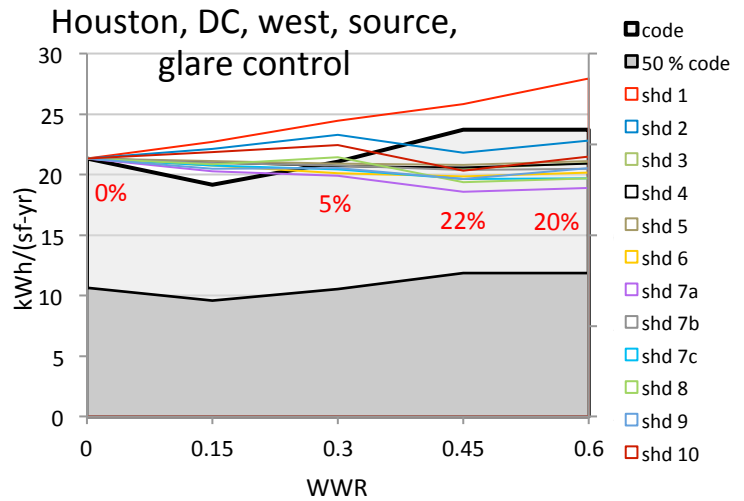


Figure 23: Total source EUI over WWR for all 12 exterior shades in Houston, west orientation, with daylighting control, with glare control. Code reference line is capped at WWR 45 %.

With daylighting control, overall savings that can be achieved through exterior shades are less, and the spread amongst the different shades is bigger than without daylighting control.

In Chicago, the use of glare control eliminates the benefit of an exterior shade for WWRs ≤ 30 % and in Houston only few exterior shades are beneficial for small to moderate windows. Glare control reduces the energy savings by 5 % (absolute savings) in Chicago compared to the case without glare control. In Houston, the impact of glare control is less pronounced with reductions of 1-2 % absolute savings for moderate to large windows.

Without glare control, the highly reflective and/or transmissive shades shd 7a, shd 8 and shd 10 (see Table 1 and Appendix B) show the lowest EUI but only shd 7a maintains its top rank when glare control is applied: shd 7a produces a comparatively moderate number of hours with discomfort glare compared to shd 8 and shd 10 (see Table 4).

With glare control, for all other exterior shades, energy savings in Chicago are either small or exterior shades are detrimental compared to the code reference case. In Houston, except for shd 1 and shd 2, energy savings range from 11-22 % for WWRs ≥ 45 %.

5. DISCUSSION

Section 3 looked at the performance of slat shading systems of varying geometry without considering discomfort glare (no additional interior shade). The simulations were run for a large window-to-wall ratio (60 %) in Chicago and Houston and for both cases, with and without daylighting control.

The prototypical building used in the simulations is internal load dominated and reducing cooling load had the biggest impact on overall energy use when no daylighting control is used. In these cases the more blocking the shades were, the lower was the energy use intensity. There was no or little negative impact on heating energy visible (e.g. on the north façade in Chicago, without daylighting control, heating energy did not increase significantly with an exterior shade), while at the same time there was a noticeable positive impact on reheat energy when cooling load was reduced (e.g. on the south façade in Chicago, without daylighting control, heating energy decreased with an exterior shade).

Without daylighting control and averaged over all orientations, all exterior shades were beneficial, and the most blocking shades performed best. A slat shading system with a cut-off angle of 0 deg (shd 5) reduced the window related energy use by 70 % in Chicago and by 96 % in Houston. Window related energy use was defined as the total energy use of the perimeter zone minus energy use (perimeter zone) for the case of a fully opaque façade.

With daylighting control, the trade-off between cooling and lighting energy lead to a minimum of energy use for a cut-off angle of 30 deg (shd 2) on the east, south and west façade for both climates, Chicago and Houston. Window related energy use was reduced by 86 % in Chicago and fully eliminated in Houston. However, when using exterior shades on the north façade with daylighting control, an increase of energy use intensity in the north perimeter zone could be seen

for most systems. Only cut-off angles > 30 deg showed still small energy savings on the north façade with daylighting control.

The results analysis did not take into account the quality of view from the inside to the outside. E.g. the most blocking shade which performed best for the case without daylighting control, does not allow for a view in horizontal direction. Architects and occupants are not likely to adopt highly blocking slat shading systems.

Section 4 looked at a variety of commercially available and frequently used exterior shading systems (roller shades, curved slats, aluminum louvers, perforated screens) in addition to the five in section 3 investigated slat shading systems. Window-to-wall ratios were varied by 15 % increments from 0 % (fully opaque façade) to 60 % (large window area). In section 4, simulations were run for a west orientation with and without glare control: when a certain value of Discomfort Glare Probability was exceeded, an interior shade was pulled and stayed down for the remainder of the day.

Without daylighting control, three shading systems with cut-off angles of 20-30 deg (shd 6, 7b, 7c) proved to be as efficient as the best performing slat shading system at 0 deg cut-off (shd 5) due to different surface properties and the shape of the shade elements. While glare control only slightly decreased the performance of the shading systems with the lowest EUI, it increased heating and cooling energy for the slat shading systems with high cut-off angle and a metal mesh (shd 1, 2 and 10).

With daylighting control, exterior shades proved to be efficient only for window-to-wall ratios of 45% and bigger, especially if glare control was applied. Whenever visual discomfort makes the use of an external shade necessary, visible light gets blocked as well, and the energy balance of lighting and cooling lead to a significant increase of EUI in the case of small windows while large windows are not as much impacted.

However, even for large windows, the energy savings through exterior shades that can be achieved with daylighting control in the Chicago climate are moderate to nil if glare control is applied. The negative impact of less available daylight on the overall heat balance (i.e. more lighting energy and additional cooling load through lights) outweighs the reduction of solar cooling load. In Houston, energy savings with exterior shades are good to moderate. The best performing shades were those with a highly reflective surface (shd 7a, 8). (Note that energy savings here refer to the code reference case that does not include glare control.)

Shades that transmit a significant portion of direct radiation performed well with daylighting control as long as there was no glare control applied. Shades that transmit a bigger portion of solar radiation through reflection, showed less frequently glare conditions and therefore they were less impacted by glare control. The simulations did not consider a loss of surface reflectance over time due to ambient conditions.

6. CONCLUSION

The simulation results showed that for the prototypical large office building with high internal loads external shades are generally beneficial and reduce window related energy and total source energy use intensity significantly. Without daylighting control and without glare control, all exterior shades can be recommended for a mixed cooling/heating climate and a hot and humid climate, for all orientations and all window-to-wall ratios, although savings are smaller for small windows and for north orientation.

In perimeter zone situations where discomfort glare plays a role, shades with high direct transmission are not recommended. The interior shade that was pulled down during glare conditions had no positive impact on overall energy use when used in combination with exterior shades. In some cases it significantly increased energy use. To reduce the impact of glare control, an automated set back (shade pulled up) could be considered.

When used in combination with daylighting controls, exterior shades can have a negative impact on the energy use intensity. With small windows or on a north façade, the loss of daylight availability increases the total energy balance. Daylighting controls without exterior shades (reference case DC) compared to the base glazing with no daylighting controls (reference case NDC) showed energy savings in the same order of magnitude as energy savings that can be achieved through exterior shades.

The simulation approach that considered glare control proved to be important in the accurate analysis of the overall energy balance which includes trade-offs between heating, cooling and lighting energy. Glare control did not only change the absolute savings that can be achieved with exterior shades, but it also changed the ranking amongst the twelve modeled variations.

It is therefore important to integrate the concept of discomfort glare and subsequent occupant behavior in building energy modeling for new construction projects. Disregarding the impact of pulled interior shades falsifies energy use predictions in particular when daylighting controls are used which is mandatory in certain states like California.

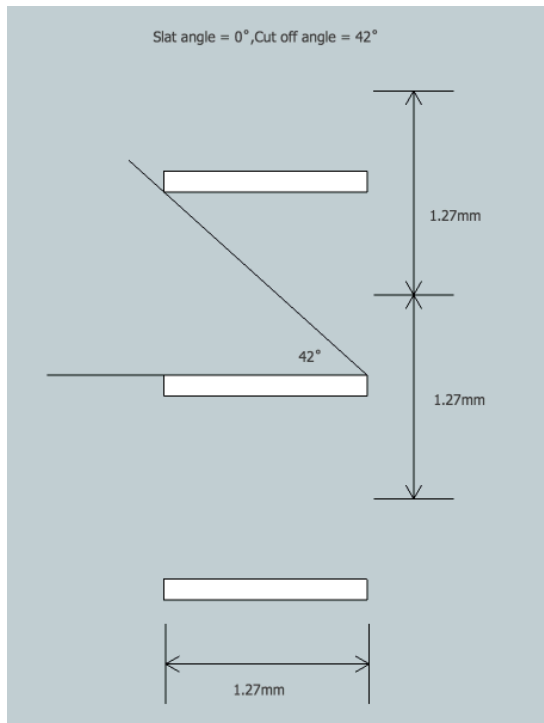
Integrating glare control into automated exterior shades could be an innovative approach. It requires manufacturers to create shading products that can provide visual comfort during glare conditions and building engineers to develop control algorithms that include the variable discomfort glare.

REFERENCES

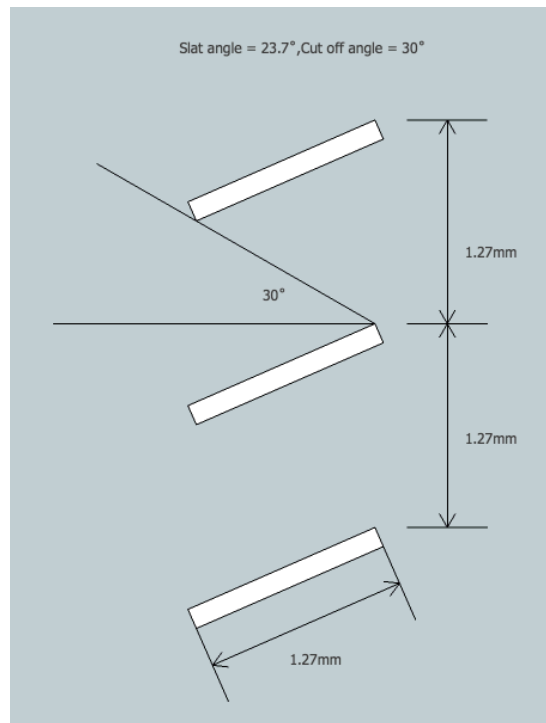
- [1] NFRC 200-2010: Procedure for Determining Fenestration Product Solar Heat Gain Coefficient and Visible Transmittance at Normal Incidence. National Fenestration Rating Council, Inc.
- [2] EN 13363-2:2005: Solar protection devices combined with glazing - Calculation of total solar energy transmittance and light transmittance - Part 2: Detailed calculation method
- [3] ASHRAE 90.1-2013: Energy Standard for Buildings Except Low-Rise Residential Buildings, published by ASHRAE

- [4] R. Mitchell, C. Kohler, J. Klems, M. Rubin, D. Arasteh, C. Huizenga, T. Yu, D. Curcija (editors), Window 6.2/ Therm 6.2 Research Version User Manual, Berkeley, CA, 2008. LBNL-941. Available at: <http://windows.lbl.gov/software/window/window.html> (accessed Jan 14, 2014).
- [5] ISO 15099-2003. Thermal Performance of Windows, Doors and Shading Devices—Detailed Calculations. Geneva: International Organization for Standardization
- [6] L. O. Grobe, S. Wittkopf, P. Apian-Bennewitz, J. C. Jonsson and M. Rubin: Experimental validation of bidirectional reflection and transmission distribution measurements of specular and scattering materials, Proc. SPIE 7725, 772510 (2010); doi:10.1117/12.854011
- [7] <http://www.koolshade.com/> (accessed Jan 8, 2014).
- [8] <http://www.clauss-markisen.de/85.0.html?&L=1> (accessed Jan 8, 2014).
- [9] http://www.warema.de/PRIVATKUNDEN/PRODUKTE/Raffstoren/Abdunkelungs_Raffstoren.php (accessed Jan 8, 2014).
- [10] <http://www.us.schott.com/architecture/english/products/daylighting-and-shading/okatech.html> (accessed Jan 8, 2014).
- [11] <http://en.sergeferrari.com/bioclimatic-facade/a-facade-for-a-new-style-of-architecture/> (accessed Jan 8, 2014).
- [12] EnergyPlus InputOutputReference.pdf, Release V8.1.08, download available: <http://apps1.eere.energy.gov/buildings/energyplus/register.cfm?goto=eplus> (accessed Jan 14, 2014).
- [13] EIA. (2005). *2003 Commercial Buildings Energy Consumption Survey*. Washington, DC: Energy Information Administration. <http://www.eia.gov/consumption/commercial/index.cfm> (accessed Jan 14, 2014).
- [14] R. Johnson, R. Sullivan, S. Nozaki, S. Selkowitz, C. Conner, D. Arasteh, Building Envelope Thermal and Daylighting Analysis in Support of Recommendations to Upgrade ASHRAE/IES Standard 90: Vol 1, Parametric Study, Analysis, and Results, Berkeley, CA, 1983. LBNL-16770. Available at http://buildings.lbl.gov/sites/all/files/16770_0.pdf, (accessed Jan 14, 2014).
- [15] http://www.energycodes.gov/development/commercial/90.1_models (accessed Jan 14, 2014).
- [16] 2013 Nonresidential Compliance Manual for the 2013 Building Energy Efficiency Standards. Title 24, Part 6, and associated. CEC-400-2013-002-CMF. California Energy Commission, Edmund G. Brown Jr., Governor
- [17] <http://bees.archenergy.com/referencemethod.html> (accessed Jan 14, 2014).
- [18] <http://radsite.lbl.gov/radiance/> (accessed Jan 24, 2014).
- [19] LL Fernandes, ES Lee, A McNeil, JC Jonsson, T Nouidui, X Pang, S Hoffmann, Angular selective window systems: Assessment of technical potential for energy savings, draft LBNL report, Jan 10, 2014
- [20] <http://www.eia.gov/consumption/commercial/data/archive/cbecs/cbecs2003/lighting/lighting1.html> (accessed Jan 24, 2014).

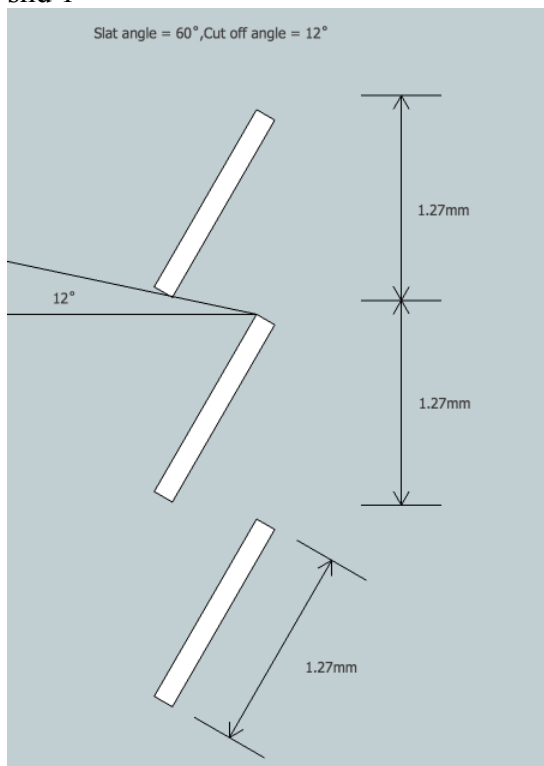
Appendix A: Geometry of exterior shades shd 1 – shd 8



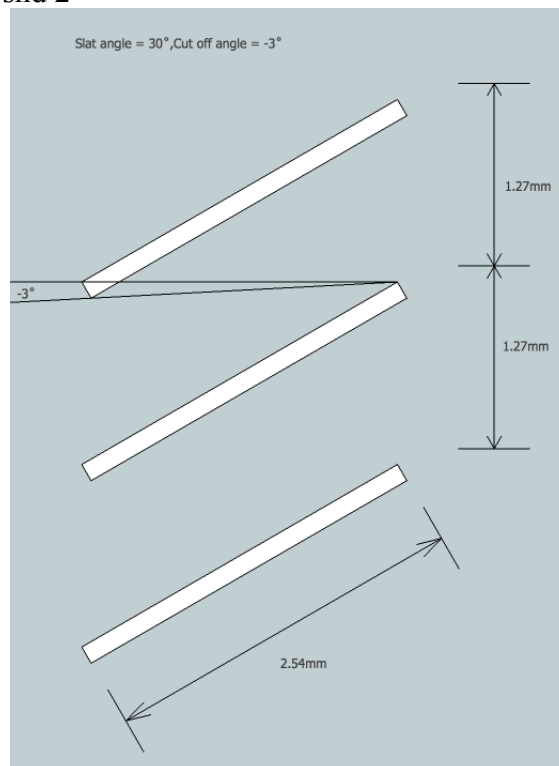
shd 1



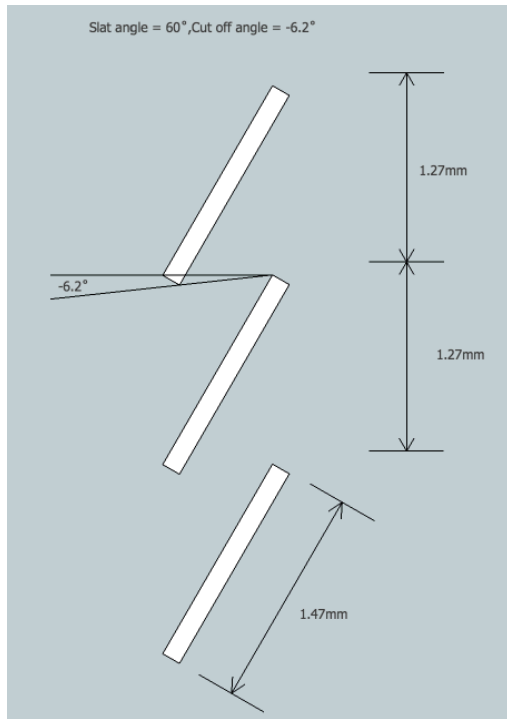
shd 2



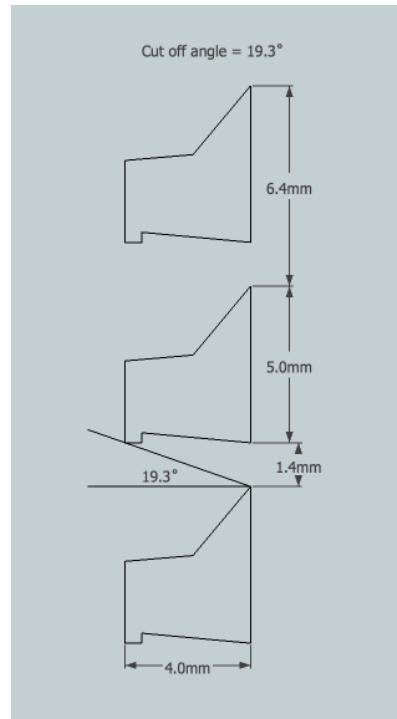
shd 3



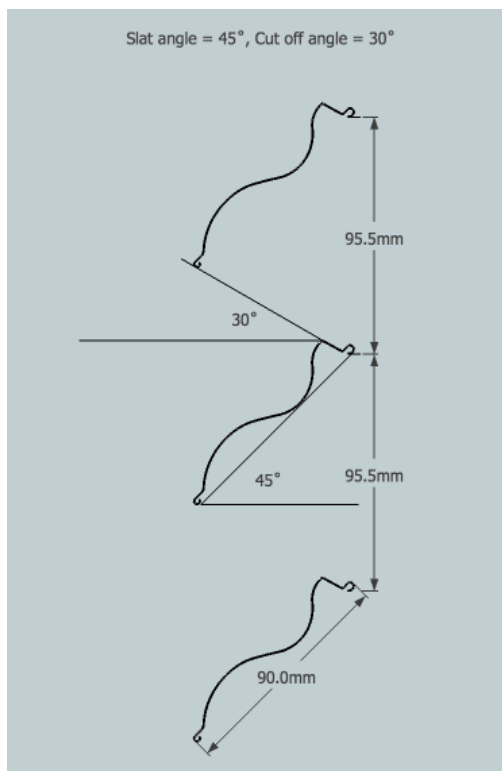
shd 4



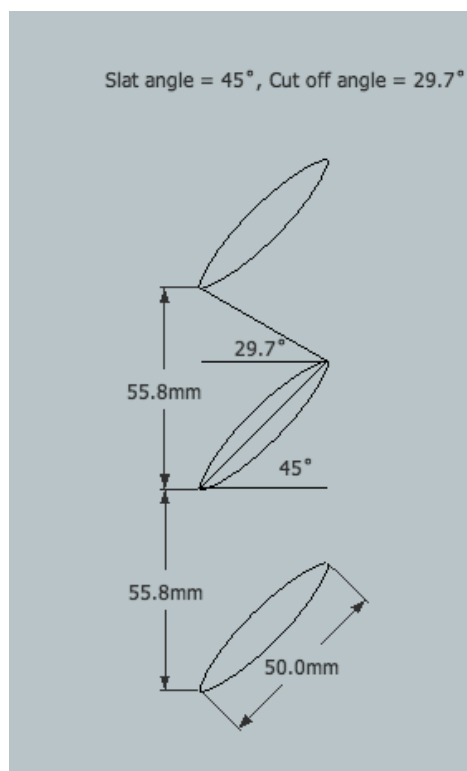
shd 5



shd 6



shd 7



shd 8

Appendix B: Simulation input for exterior shading systems shd 1 – shd 10

Name	Distance from glass [mm]	Thickness of system [mm]	Material Conductivity [W/mK]	Shade Conductance [W/mK]	Front Opening Multiplier [-]	Cut-off angle [deg]
INTERIOR SHADE						
Interior Shade	50	1.0	0.15	0.15	0.03	n.a.
EXTERIOR SHADE						
shd 1	13	1.3	15	0.17	0.99	45
shd 2	13	1.1	15	2.12	0.86	30
shd 3	13	0.6	15	7.51	0.5	15
shd 4	13	2.5	15	2.12	0.86	0
shd 5	13	0.5	15	7.51	0.5	0
shd 6	50	4	15	11.6	0.23	20
shd 7a, 7b, 7c	50	42	150	46.5	0.69	30
shd 8	50	42	150	46.5	0.69	30
shd 9	500	1.0	(0.20)	0.15	0.28	n.a.
shd 10	500	5.0	(0.65)	20	0.4	n.a.

Table B1: Properties of the shading systems and simulation input values

Name	IR Transmittance [-]	Material Emissivity [-] x	Shade Emittance [-]	Top Opening Multiplier [-]	Right/Left Opening Multiplier [-]	Bottom Opening Multiplier [-]
INTERIOR SHADE						
Interior Shade	0.03	0.90	0.873	0	0.5	0.5
EXTERIOR SHADE						
shd 1	0.52	0.5	0.37	0	0	0
shd 2	0.45	0.5	0.38	0	0	0
shd 3	0.27	0.5	0.43	0	0	0
shd 4	0.26	0.5	0.55	0	0	0
shd 5	0.27	0.5	0.43	0	0	0
Shd 6	0.23	0.6	0.46	0.25	0.5	0.5
shd 7a	0.5	0.1	0.085	0.25	1	1
shd 7b, 7c	0.41	0.5	0.38	0.25	1	1
shd 8	0.5	0.1	0.085	1	1	1
shd 9	0.29	-	0.29	0.25	0.25	0.25
shd 10	0.371	-	0.114	0.25	0.25	0.25

Table B2: Properties of the shading systems and simulation input values

Name	Diffuse Solar Reflectance [-]	Total Solar Reflectance [-]	Diffuse Visible Reflectance [-]	Total Visible Reflectance [-]
INTERIOR SHADE				
Interior Shade*	0.75	0.75	0.75	0.75
EXTERIOR SHADE				
shd 1	0.5	0.5	0.5	0.5
shd 2	0.5	0.5	0.5	0.5
shd 3	0.5	0.5	0.5	0.5
shd 4	0.5	0.5	0.5	0.5
shd 5	0.5	0.5	0.5	0.5
Shd 6	0.4	0.55	0.41	0.6
shd 7a	0.93	0.93	0.87	0.87
shd 7b	0.08	0.08	0.15	0.15
shd 7c	0.56	0.56	0.4	0.4
shd 8	0.7	0.7	0.7	0.7
shd 9*	0.3	0.3	0.3	0.3
shd 10*	0.38	0.38	0.38	0.38

Table B3: Material reflectance (*shade reflectance)